Journal of Applied Polymer Science

High-performing dye-sensitized solar cells based on reduced graphene oxide/PEDOT-PSS counter electrodes with sulfuric acid post-treatment

Zhang Lan, Suwen Gao, Jihuai Wu, Jianming Lin

Engineering Research Center of Environment-Friendly Functional Materials, Ministry of Education, Key Laboratory of Functional Materials for Fujian Higher Education, Institute of Materials Physical Chemistry, Huaqiao University, Xiamen 361021, China

Correspondence to: Z. Lan (E-mail: lanzhang@hqu.edu.cn)

ABSTRACT: Four kinds of counter electrodes are prepared with polystyrene-sulfonate doped poly(3,4-ethylenedioxythiophene) (PEDOT-PSS) as basic material, reduced graphene oxide (rGO) sheets as additives and H_2SO_4 as treating agent. The cyclic voltammetry and Tafel polarization are measured to evaluate catalytic activity of these counter electrodes for I_3^-/I^- redox couple. It is found that H_2SO_4 treated rGO and PEDOT-PSS hybrid counter electrode (S/rGO/PEDOT-PSS counter electrode) has the highest catalytic activity among these counter electrodes. Power conversion efficiency of the dye-sensitized solar cell with S/rGO/PEDOT-PSS counter electrode can attain to 7.065%, distinctly higher than that of the cells with the other three ones, owing to the great enhanced fill factor and short-circuit current density. © 2015 Wiley Periodicals, Inc. J. Appl. Polym. Sci. **2015**, *132*, 42648.

KEYWORDS: applications; batteries and fuel cells; functionalization of polymers; graphene and fullerenes; nanotubes

Received 25 April 2015; accepted 22 June 2015

DOI: 10.1002/app.42648

INTRODUCTION

As a kind of low-cost and environment-friendly solar cells, dye-sensitized solar cells (DSSCs) have attracted many attentions in the past decades.[1] A typical DSSC has three components as a dye-sensitized photoelectrode, a counter electrode, and an electrolyte.[2] Among them, the counter electrode acts as a key role in reducing redox species [usually using tri-iodide/iodide (I_3^-/I^-) redox couple] used to regenerate the oxidized dyes. To accelerate the reduction reaction, a catalyst is often needed because the transparent conducting oxide glass has not catalytic activity.[3] Platinum has been proved as one of the most active catalysts.[4] However, it is very expensive and cannot meet the low-cost characteristic of DSSCs. Therefore, other cheaper substitutes have been used to fabricate low-cost counter electrodes.[5–7]

As one important conductive polymer, polystyrene-sulfonate doped poly (3,4-ethylenedioxythiophene) (PEDOT-PSS) has some special characteristics such as high conductivity, transparency, environmental stability, and good film-forming ability. Therefore, it becomes a good material for preparing low-cost counter electrodes of DSSCs.[8–10] However, owing to low conductivity of pristine PEDOT-PSS (below 1 S cm^{-1}), performance of the counter electrode with pristine PEDOT-PSS is very poor.[11] The limitation can be improved by two ways. One is incorporating some highly conductive and active catalysts in PEDOT-PSS. For example, graphene, which consists of a two-dimensional sheet of covalently bonded carbon atoms and has unique electronic property and strong catalytic activity,[8] is a good candidate. The other is treating PEDOT-PSS with some special solvents such as ethylene glycol, glycerol, sorbitol, alcohol, sulfuric acid (H_2SO_4), and so on, to enhance the conductivity.[12–15]

Here, reduced graphene oxide (rGO) sheets are selected as functional additives to form rGO/PEDOT-PSS hybrid counter electrode. Furthermore, H_2SO_4 is used to treat the counter electrode, which results in significantly enhanced catalytic activity of the counter electrode and photovoltaic performance of the DSSC.

EXPERIMENTAL

Materials

Tetrabutyl ammonium iodide, acetonitrile, PEDOT-PSS (1.3-1.7 wt %), H_2SO_4, graphite, 4-tert-butyl pyridine, $NaBH_4$, NaI, I_2, LiI, $LiClO_4$, and $H_2PtCl_6{\cdot}6H_2O$ were all A. R. grade and purchased from Sinopharm Chemical Reagent, China. The reagents were used without further treatment. Conducting glasses (FTO glasses, Fluorine doped tin oxide over-layer, sheet resistance 15 $\Omega{\cdot}square^{-1}$, purchased from Nippon Glass) were used as substrates for preparing photograph and counter electrodes. Sensitizing dye N719 {*cis*-$[(dcbH_2)_2Ru(SCN)_2]^{2-}$, $2(n\text{-}C_4H_9)_4N^+$ ($dcbH_2$ = 2,2′-bipyridine-4,4′-dicarb oxylic acid)} was purchased from Dye sol.

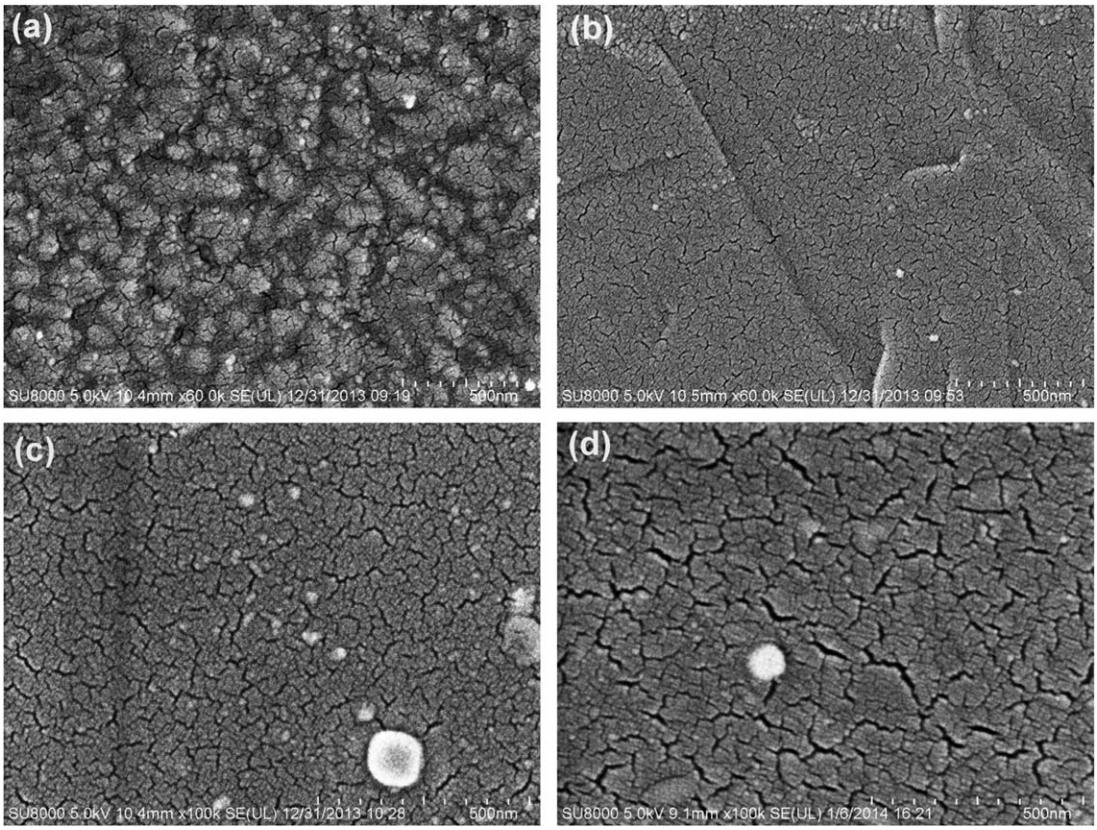

Figure 1. SEM images of the four kinds of counter electrodes. (a) PEDOT-PSS, (b) S/PEDOT-PSS, (c) rGO/PEDOT-PSS, and (d) S/rGO/PEDOT-PSS.

Preparation of PEDOT-PSS Based Counter Electrodes

Graphene oxide (GO), prepared with modified hummer method,[16] was added into PEDOT-PSS with concentration of 1 mg ml^{-1}. After ultrasonic treatment at least 10 h, the well dispersed solution was spread out on FTO glasses with doctor blade method. The GO/PEDOT-PSS coated FTO glasses were dried at 80°C for 0.5 h, and then immersed in 0.1*M* $NaBH_4$ solution for 1 h to turn GO to rGO in the composite film. After rinsed with deionized water three times and dried, rGO/PEDOT-PSS counter electrodes were obtained. H_2SO_4 treated counter electrodes (marked as S/PEDOT-PSS and S/rGO/PEDOT-PSS) were made by dipping PEDOT-PSS and rGO/PEDOT-PSS counter electrodes in 1*M* H_2SO_4 solution for 0.5 h, rinsing with deionized water three times and drying. Pt counter electrode was prepared by heating a FTO glass coated with a drop of Pt precursor solution (containing 5 mg $H_2PtCl_6{\cdot}6H_2O$ and 1 ml 2-propanol) at 400°C for 30 min.

Preparation of DSSCs

The front-side illuminated photoelectrodes based on ordered TiO_2 nanotube arrays are fabricated according to our former reported methods.[17] Briefly, membranes of TiO_2 nanotube arrays are prepared with anodic oxidation of polished Ti foils at 60 V for 4 h. After detached from Ti foils, the membranes are adhered to FTO glasses using the paste containing 10–20 nm anatase TiO_2 nanoparticles. Before soaking in N719 dye solution, the membranes on FTO glasses are treated with $TiCl_4$ aqueous solution and 450°C high temperature sintering. Finally, the N719 dye sensitized front-side illuminated photoelectrodes based on ordered TiO_2 nanotube arrays are obtained after 24 h immersing in the dye solution at room temperature. The DSSCs were assembled by dripping a drop of electrolyte on a dye-sensitized TiO_2 nanotube arrays based photoelectrode. A piece of as-prepared counter electrodes was placed above it. The two electrodes were clipped together and a cyanoacrylate adhesive was used as sealant to seal the solar cell. Bisphenol A epoxy resin was used in a further sealing process. The liquid electrolyte contains 0.4*M* sodium iodide, 0.1*M* tetrabutyl ammonium iodide, 0.5*M* 4-tert-butylpyridine, and 0.05*M* iodine in acetonitrile solution.

Measurements

The morphologies of counter electrodes were analyzed by a field emission scanning electron microscopy (SU8000, HITACHI). The CHI 660 C electrochemical workstation was used to carry out the cyclic voltammetry (CV) and Tafel polarization measurements. CV measurement of I_3^-/I^- redox couple at counter electrodes was done in an acetonitrile solution containing 0.01*M* LiI, 0.001*M* I_2, and 0.1*M* $LiClO_4$ with three-electrode system using the as-prepared counter electrodes as working electrodes, Pt foil as counter electrode and Ag/AgCl as reference electrode. A symmetrical cell (CE/electrolyte/CE) was assembled with the two pieces of identical counter electrodes and filled with liquid electrolyte the same as that used in DSSCs for Tafel polarization test. The Tafel polarization test was measured under dark condition at room temperature, and the scanning potential range was from −1 to 1 V with rate of 10 mV s^{-1}. The photovoltaic tests of DSSCs were carried out by measuring

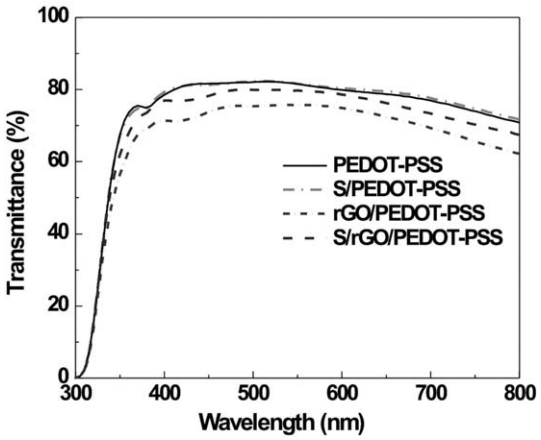

Figure 2. Transmittance of the four kinds of counter electrodes.

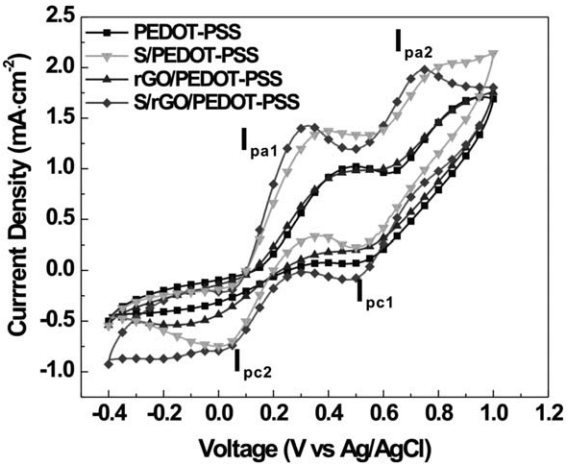

Figure 4. CV curves of four kinds of counter electrodes, at scan rate of 50 mV S^{-1}.

the photocurrent-voltage (J-V) characteristic curves under simulated AM 1.5 G solar illumination at 100 mW cm^{-2} with #94043A solar simulator (PVIV-94043A, Newport). All of the samples were tested five times and the average data were taken. The active area of DSSCs was 0.12 cm^2 (0.3 × 0.4 cm^2).

RESULTS AND DISCUSSION

Figure 1 shows morphologies of PEDOT-PSS, S/PEDOT-PSS, rGO/PEDOT-PSS, and S/rGO/PEDOT-PSS counter electrodes. From the figures, it is observed that the counter electrodes have large numbers of nanocracks, which can come into well contact with electrolyte in the DSSC and enhancing catalytic activity.[10] The addition of rGO sheets in the counter electrode brings about bigger nanocracks. Furthermore, the films become more homogeneous after H_2SO_4 treatment, which results in higher transparency compared with the nontreated ones as shown in Figure 2.

From Figure 3(a), we can see that the GO sheet is extremely thin with area about 0.3 μm^2. Figure 3(b) shows Raman spectra of GO, rGO/PEDOT-PSS, and PEDOT-PSS films. The G band (E_{2g} mode of sp^2 carbon atoms) and the D band (symmetry A_{1g} mode) of GO locate at 1596 and 1352 cm^{-1}, respectively. After reduction with $NaBH_4$ solution, the G band of rGO blue shifts to 1571 cm^{-1}, which is consistent with the results of rGO.[18] Moreover, the intensity ratio of D band to G band (I_D/I_G) increases, indicating the decrease of average size of sp^2 domains on rGO.[19] The band between 1400 and 1500 cm^{-1} corresponds to the stretching vibration of C_α=C_β on the five-member ring of PEDOT.[20] All of these characteristics suggest that the rGO sheets are formed in rGO/PEDOT-PSS counter electrode.

The CV measurement is done and shown in Figure 4 for investigating the catalytic activity of the four kinds of counter electrodes for reducing I_3^- to I^-. We can see that the CV patterns have similar morphologies, which contain two anodic current peaks and two cathodic current peaks. The four peaks in the patterns are related to the oxidation of I^- ions and the reduction of I_3^- ions (I_{pa1}: $3I^- = I_3^- + 2e^-$, I_{pa2}: $2I_3^- = 3I_2 + 2e^-$, I_{pc1}: $3I_2 + 2e^- = 2I_3^-$, I_{pc2}: $I_3^- + 2e^- = 3I^-$).[21] The cathodic peak current at more negative potential (I_{pc2}) in the CV curve indicates the catalytic activity of counter electrode for I_3^- reduction. It is shown that rGO/PEDOT-PSS counter electrode has a higher I_{pc2} value than that of PEDOT-PSS counter electrode. After H_2SO_4 treatment, the I_{pc2} values of the two counter electrodes all increase, and the S/rGO/PEDOT-PSS counter electrode shows a little higher value than that of S/PEDOT-PSS counter electrode. Furthermore, the H_2SO_4 treatment also decreases the peak-to-peak separation voltage values (from I_{pa1} to I_{pc2} in the CV patterns) of both S/rGO/PEDOT-PSS and S/PEDOT-PSS counter

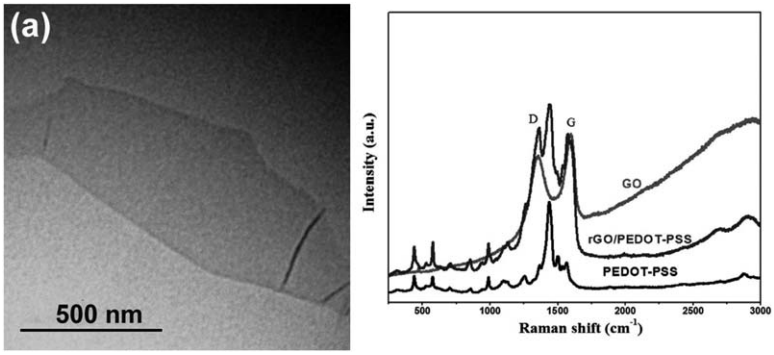

Figure 3. TEM image of GO (a); and Raman spectra of GO, S/ rGO/PEDOT-PSS, and PEDOT-PSS (b).

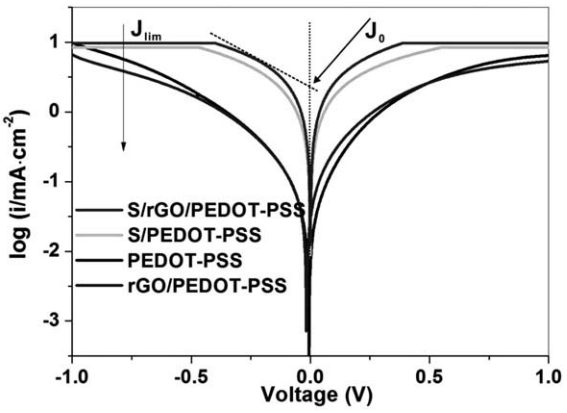

Figure 5. Tafel polarization curves of four kinds of dummy cells fabricated with two identical counter electrodes.

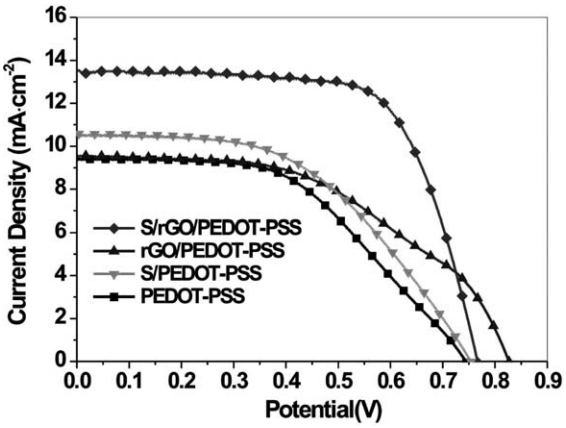

Figure 6. J-V curves of DSSCs with four kinds of counter electrodes.

electrodes compared with their non-treated counterparts, and the peak-to-peak separation voltage value of S/rGO/PEDOT-PSS counter electrode is lower than that of S/PEDOT-PSS counter electrode. So it can be verified that S/rGO/PEDOT-PSS counter electrode has the highest catalytic activity for reducing I_3^- among the four counter electrodes.[22]

Tafel polarization curves are measured to examine the interfacial charge transfer properties of the I_3^-/I^- couple at the counter electrodes. Figure 5 is the logarithmic current density as a function of the voltage for the reduction of I_3^- to I^-, from which we can obtain the two important parameters, as the exchange current density (J_0) and the limiting diffusion current density (J_{lim}), relating to the catalytic activity of counter electrodes.[23] It is seen that the H_2SO_4 treatment causes obviously increased J_0 and J_{lim} values of S/rGO/PEDOT-PSS and S/PEDOT-PSS counter electrodes. The bigger J_0 value means the higher catalytic activity. Moreover, according to the equation of $D = J_{lim}L/(2nFC)$,[24] where D is the diffusion coefficient of the I_3^-, L is the diffusion length of I_3^- in the symmetric cell, and the pores of measured counter electrodes. C is the I_3^- concentration, F is the Faraday constant, J_{lim} is proportional to the diffusion properties of the I_3^-/I^- couple, so S/rGO/PEDOT-PSS counter electrode has the fastest I_3^-/I^- diffusion rate among the four kinds of counter electrodes.

Figure 6 shows the J-V curves of DSSCs with the four counter electrodes. The photovoltaic parameters are summarized in Table I. It is seen that the DSSC with S/rGO/PEDOT-PSS counter electrode shows distinctly higher power conversion efficiency (PCE) than that of the cell with the other three ones, owing to the prominently larger fill factor (FF) and short-circuit current density (J_{sc}). As aforementioned, the highest J_0 and J_{lim} values of S/rGO/PEDOT-PSS counter electrode can cause the lowest diffusion resistance of the DSSC compared with the other three ones, which results in the highest FF.[25] Furthermore, the related data reveal that S/rGO/PEDOT-PSS counter electrode has the highest catalytic activity, which is beneficial for the fast light-to-electricity conversion processes, so the cell shows high J_{sc} values.

CONCLUSIONS

To increase the catalytic activity of PEDOT-PSS based counter electrodes and photovoltaic performance of DSSCs, GO sheets are added into the PEDOT-PSS film and *in-situ* reduced with $NaBH_4$. The hybrid film is further treated with 1*M* H_2SO_4 aqueous solution. It is found that the addition of rGO sheets into the PEDOT-PSS film can form bigger nanocracks and the further H_2SO_4 treatment results in more homogeneous surface morphology and higher transparency compared with the pure PEDOT-PSS film. The Raman spectra verify the successful reduction of GO sheets to rGO in the hybrid film. The CV data show that the addition of rGO in the PEDOT-PSS film combining with H_2SO_4 treatment both can increase the catalytic activity. The Tafel polarization data confirm the positive influences of rGO sheets and H_2SO_4 treatment on the catalytic activity of the PEDOT-PSS film again. PCE of DSSCs with H_2SO_4 treated rGO/PEDOT-PSS film can attain to the highest value about 7.065% compared with other three kinds of PEDOT-PSS based counter electrodes.

Table I. Photovoltaic Parameters of DSSCs Shown in Figure 6

Counter electrode	Voc (V)	Jsc (mA cm^{-2})	FF	PCE (%)
PEDOT-PSS	0.745 ± 0.003	9.397 ± 0.013	0.505 ± 0.002	3.535 ± 0.034
S/PEDOT-PSS	0.754 ± 0.005	10.471 ± 0.014	0.503 ± 0.003	3.971 ± 0.056
rGO/PEDOT-PSS	0.827 ± 0.002	9.554 ± 0.018	0.499 ± 0.005	3.943 ± 0.056
S/rGO/PEDOT-PSS	0.767 ± 0.006	13.486 ± 0.017	0.683 ± 0.003	7.065 ± 0.095

ACKNOWLEDGMENTS

This work was supported by the National Natural Science Foundation of China (Nos. U1205112, 51002053, and 61474047), the Key Project of the Chinese Ministry of Education (212206), the Fujian Provincial Science Foundation for Distinguished Young Scholars (2015J06011), the Programs for Prominent Young Talents and New Century Excellent Talents in Fujian Province University, and the Promotion Program for Yong and Middle-aged Teacher in Science and Technology Research of Huaqiao University (ZQN-YX102).

REFERENCES

1. O' Regan, B.; Grätzel, M. *Nature* **1991**, *353*, 737.
2. Grätzel, M. *J. Photochem. Photobiol. C* **2003**, *4*, 145.
3. Thomas, S.; Deepak, T. G.; Anjusree, G. S.; Arun, T. A.; Nair, S. V.; Nair, A. S. *J. Mater. Chem. A* **2014**, *2*, 4474.
4. Fang, X.; Ma, T.; Guan, G.; Akiyama, M.; Kida, T.; Abe, E. *J. Electroanal. Chem.* **2004**, *570*, 257.
5. Li, Q.; Wu, J.; Tang, Q.; Lan, Z.; Li, P.; Lin, J.; Fan, L. *Electrochem. Commun.* **2008**, *10*, 1299.
6. Yun, S.; Hagfeldt, A.; Ma, T. *Adv. Mater.* **2014**, *26*, 6210.
7. Menaka, C.; Manisankar, P.; Stalin, T. *J. Appl. Polym. Sci.* **2015**, *132*, 42041.
8. Hong, W.; Xu, Y.; Lu, G.; Chun, Li; Shi, G. *Electrochem. Commun.* **2008**, *10*, 1555.
9. Chen, J. G.; Wei, H. Y.; Ho, K. C. *Sol. Energy Mater. Sol. Cells* **2007**, *91*, 1472.
10. Gao, S.; Lan, Z.; Wu, W.; Que, L.; Wu, J.; Lin, J. *Polym. Adv. Technol.* **2014**, *25*, 1560.
11. Xu, S.; Luo, Y.; Liu, G.; Qiao, G.; Zhong, W.; Xiao, Z.; Luo, Y.; Ou, H. *Electrochimi. Acta* **2015**, *156*, 20.
12. Kim, Y. H.; Sachse, C.; Machala, M. L.; May, C.; Meskamp, L. M.; Leo, K. *Adv. Funct. Mater.* **2011**, *21*, 1076.
13. Huang, J.; Li, G.; Yang, Y. *Adv. Mater.* **2008**, *20*, 415.
14. Bounioux, C.; Katz, E. A.; Yerushalmi-Rozen, R. *Polym. Adv. Technol.* **2012**, *23*, 1129.
15. Kim, N.; Kee, S.; Lee, S. H.; Lee, B. H.; Kahng, Y. H.; Jo, Y. R.; Kim, B. J.; Lee, K. *Adv. Mater.* **2014**, *26*, 2268.
16. Marcano, D. C.; Kosynkin, D. V.; Berlin, J. M.; Sinitskii, A.; Sun, Z. Z.; Slesarev, A.; Alemany, L. B.; Lu, W.; Tour, J. M. *ACS Nano* **2010**, *4*, 4806.
17. Gao, S.; Lan, Z.; Wu, W.; Que, L.; Wu, J.; Lin, J.; Huang, M. *Acta Phys. Chim. Sin.* **2014**, *30*, 446.
18. Stankovich, S.; Dikin, D. A.; Piner, R. D.; Kohlhaas, K. A.; Kleinhammes, A.; Jia, Y. Y.; Wu, Y.; Nguyen, S. T.; Ruoff, R. S. *Carbon* **2007**, *45*, 1558.
19. Gao, W.; Alemany, L. B.; Ci, L. J.; Ajayan, P. M. *Nat. Chem.* **2009**, *1*, 403.
20. Garreau, S.; Duvail, J. L.; Louarn, G. *Synth. Met.* **2002**, *125*, 325.
21. Gong, F.; Wang, H.; Xu, X.; Zhou, G.; Wang, Z. S. *J. Am. Chem. Soc.* **2012**, *134*, 10953.
22. Zhang, X.; Yang, Y.; Guo, S.; Hu, F.; Liu, L. *ACS Appl. Mater. Interfaces* **2015**, *7*, 8457.
23. Wu, M.; Lin, X.; Hagfeldt, A.; Ma, T. *Angew. Chem. Int. Ed.* **2011**, *50*, 3520.
24. Wang, M.; Anghel, A. M.; Marsan, B.; Ha, N. C.; Pootrakulchote, N.; Zakeeruddin, S. M.; Grätzel, M. *J. Am. Chem. Soc.* **2009**, *131*, 15976.
25. Pysch, D.; Mette, A.; Glunz, S. W. *Sol. Energy Mater. Sol. C* **2007**, *91*, 1698.